Estimates of Nonequilibrium Radiation for Venus Entry

WILLIAM L. GROSE* AND JOHN E. NEALY†
NASA Langley Research Center, Hampton, Va.

The present investigation is an analysis of the radiation from the chemical nonequilibrium region in the shock layer about a vehicle during Venus entry. The radiation and the flow were assumed to be uncoupled. An inviscid, nonequilibrium flowfield was calculated and an effective electronic temperature was determined for the predominant radiating species. Species concentrations and electronic temperature were then input into a radiation transport code to calculate heating rates. The present results confirm earlier investigations which indicate that the radiation should be calculated using electronic temperatures for the radiating species. These temperatures are not related in a simple way to the local translational temperature. For the described mission, the nonequilibrium radiative heating rate is approximately twice the corresponding equilibrium value at peak heating.

Nomenclature

g = degeneracy of electronic energy state
h = enthalpy
k = Boltzmann constant
K = equilibrium constant
k_{r_e} = backward rate constant for electrons in Eq. (3)
k_{r_m} = backward rate constant for heavy particles in Eq. (3)
$[M]$ = number density of general species, M
n = number density
q^c = convective heat transfer rate
q^r = radiative heat transfer rate
$q_o{}^r$ = radiative heat transfer rate calculated with radiation-less properties
Q = spectral flux
r = distance from body axis of symmetry
R_b = base radius of body
R_n = nose radius of body
t = time
T = translational temperature
T_e = electronic temperature
V = velocity
x = curvilinear distance along shock wave
y = normal distance from shock
z = distance along body symmetry axis
Γ = radiation—convection parameter, $\dfrac{q_o{}^r}{\rho_\infty V_\infty h_s}$
γ_E = entry angle
e = energy of electronic state
θ_c = cone half-angle
λ = radiative transition rate/molecule
ρ = density

Subscripts

eq = equilibrium
ne = nonequilibrium
o = ground electronic state
s = stagnation conditions
w = wall conditions
∞ = freestream conditions

Superscripts

$*$ = $A^1\pi$ (fourth positive group) electronic state of CO

Introduction

THE flow in the shock layer that forms about a high-speed vehicle entering a planetary atmosphere may experience a severe departure from chemical equilibrium. Heating studies[1,2] that preceded the Apollo flights indicated that the radiation from the nonequilibrium region of the shock layer was several times that predicted by an equilibrium analysis for certain conditions during earth entry. However, these conditions occurred at high altitudes where the radiative heating contributed only a small portion of the total heating. The present investigation was undertaken to estimate the nonequilibrium radiation for conditions that might be typical of a Venusian entry.

Various papers exist dealing with the high-temperature chemistry and radiative properties of CO_2 and CO_2–N_2 systems.[3-5] Reference 3 summarizes some of the more important reaction rates in a CO_2–N_2 system but does not include the important radiative processes taking place in the far ultraviolet spectral region. References 4 and 5 include more of the significant radiative processes but analyze radiative behavior of CO_2–N_2 mixtures with large nitrogen content (40–75%). Even though Ref. 5 deals largely with nonequilibrium radiation from the CN violet band system, an indication is given of the increase in radiant emission due to chemical nonequilibrium effects.

An unmanned, scientific mission currently under consideration involves a multiprobe entry of one large and three small sphere-cone bodies released from a spacecraft.[6,7] Trajectories for the large probe and the small probe having the steepest entry angle are shown in Fig. 1. To date, the analysis has been completed for the large probe and the following discussion is limited to those results.

Analysis

The analysis was conducted in the following manner. The flow and the radiation were assumed to be uncoupled. The criterion for uncoupling is that the radiation-convection parameter

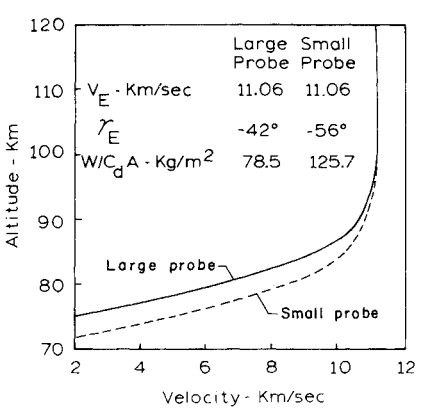

Fig. 1 Trajectory for Venus Probe.

Received March 13, 1974; revision received September 16, 1974.
Index category: Radiation and Radiative Heat Transfer.
* Aerospace Research Scientist. Member AIAA.
† Aerospace Research Scientist.

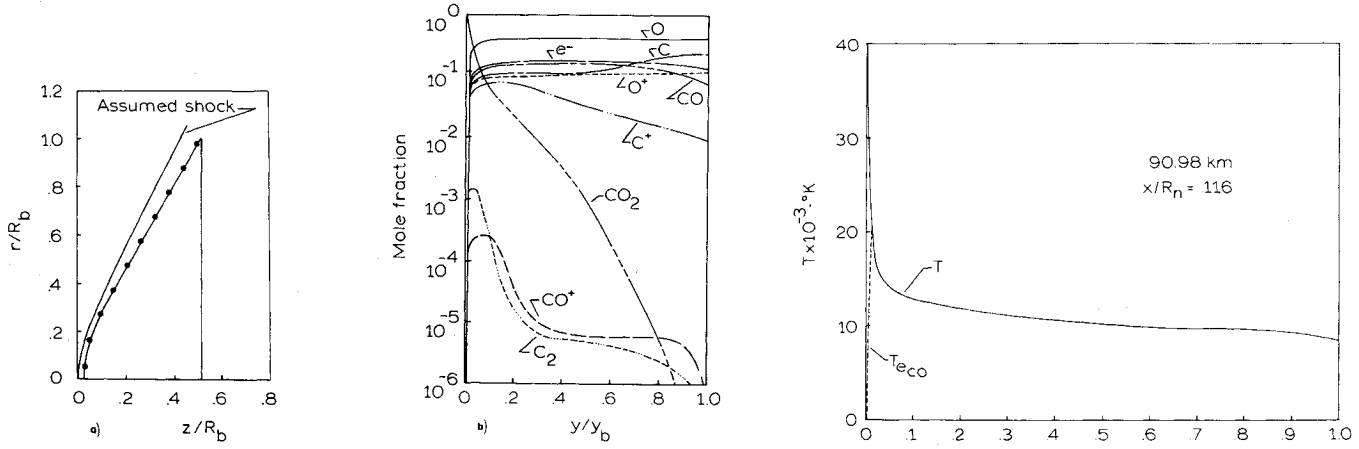

Fig. 2a) Computed body points, desired 60° half-angle cone, $R_b = 0.6858$, $R_n/R_b = 0.5$ m. Assumed shock and computed body, 90.98 km; b) species concentration profiles across shock layer, $x/R_n = 0.116$; c) temperature profiles across shock layer.

$$\Gamma = q_o^r/\rho_\infty V_\infty h_s \tag{1}$$

cited by Goulard[8] satisfy the restriction, $\Gamma \ll 1$. For the trajectory points considered in this investigation this criterion was satisfied. An inverse, nonequilibrium, inviscid flowfield computer code[9] was used to calculate the flow variables and species concentrations at four altitudes (88.22, 90.98, 92.40, and 96.72 km). The flowfield code is based upon the thin-shock-layer approximations of Maslen.[10] An approximate pressure distribution is determined and the chemical rate equations are integrated along streamlines.

Current evidence[11] suggests the Venus atmosphere is largely CO_2 with at most 3% N_2 and water vapor by volume. Therefore, for the purpose of this preliminary study, an atmosphere of 100% CO_2 was assumed. Table 1 illustrates the reaction mechanism considered for the investigation. After some preliminary calculations it was decided that two charge formation reactions (reactions 11 and 12) and two charge exchange reactions (reactions 13 and 14) could be deleted without compromising the results of this work. The reaction rates used were obtained from Refs. 12 and 13. Experimental observation of C_2 radiation in shock tube studies[14] of Venus entry indicated a nonequilibrium overshoot near the shock front. Early calculations using the more conventional reaction

$$C_2 + M \rightleftarrows 2C + M \tag{2}$$

instead of reaction 4 (Table 1) did not indicate a C_2 overshoot. When reaction 4 was included using a rate constant calculated by collision theory the C_2 nonequilibrium overshoot was predicted. The actual mechanism for this overshoot is undoubtedly more complex and may consist of numerous steps; however, the simple reaction 4 proposed here, predicts the experimentally observed behavior.

Results from the nonequilibrium, inviscid flow calculations at 90.98 km are presented in Fig. 2a. The computed body shape is seen to closely approximate the 60° half-angle sphere-cone described by the parameters on the figure. Profiles of species concentrations across the shock-layer in the stagnation region at $x/R_n = 0.116$ are shown in Fig. 2b. The CO concentration increases rapidly and remains approximately constant over 95% of the shock layer thickness. Subsequent analysis indicated that the radiation from the nonequilibrium zone near the shock front was dominated by the fourth positive band system of CO. The previously described C_2 overshoot is also observed in this figure.

Hansen et al.[15] pointed out the fallacy of assuming that excited electronic states are populated according to a Boltzmann distribution characterized by the translational temperature of the gas for high-temperature nonequilibrium shock layers. In the investigation of Ref. 15, this assumption resulted in total calculated radiation about two orders of magnitude higher than observed values due to the contribution from the thin layer near the shock front where the temperature is very high. Subsequent preliminary radiation calculations for the present investigation substantiated this conclusion. Following the model of Ref. 15, the two-body collision of molecular species was assumed to be the predominant mechanism for exciting electronic states. For the reaction

$$CO + M \leftrightarrows CO^* + M \tag{3}$$

The production rate of CO* can be written

$$\frac{dn_{CO}^*}{dt} = \frac{g_o}{g_o + g^*}\{k_{r_m} K n_{CO}[M] - k_{r_m} n_{CO}^*[M] + k_{r_e} - K n_{CO} n_{e^-} - k_{r_e^-} n_{CO}^* n_{e^-}\} - n_{CO}^* \lambda_{CO} \tag{4}$$

For all species except electrons, the backward rate constant is calculated from collision theory to be

$$k_{r_m} = 1.9(10^{-36})T^{1/2} \text{ cm}^3/\text{sec} \tag{5}$$

For electrons

$$k_{r_e^-} = 6.2(10^{-12})T^{1/2} \text{ cm}^3/\text{sec} \tag{6}$$

Equation (4) was integrated using an implicit (trapezoidal rule) finite difference technique with the assumption that the inviscid flowfield output yielded the correct ground state populations. Assuming a Boltzmann distribution among the excited electronic states, an effective electronic temperature for CO is determined from the relation

$$\frac{n_{CO}^*}{n_{CO}} = g^* \exp\left(\frac{-e^*}{kT_{e_{CO}}}\right) \Big/ \sum_i g_i \exp\left(\frac{-e_i}{kT_{e_{CO}}}\right)$$

The variation of T and $T_{e_{CO}}$ across the shock layer at $x/R_n = 0.116$ is shown in Fig. 2c. The $T_{e_{CO}}$ profile overshoots near the shock front and then quickly reaches equilibrium with T.

The radiative properties of the shock layer were calculated using the radiative transport code of Ref. 16. This code allows consideration of a nongray gas with molecular band, continuum, and atomic line transitions. A detailed frequency dependence of absorption coefficients is used to integrate over the radiation spectrum and a tangent slab approximation is used to integrate over physical space. Radiative heating rates to the body were calculated with the radiative transport code using the non-

Table 1 Reaction mechanism

1) $CO_2 + M = CO + O + M$	8) $CO + C^+ = CO^+ + C$
2) $CO + M = C + O + M$	9) $CO + O^+ = CO^+ + O$
3) $O_2 + M = 2O + M$	10) $O + C^+ = O^+ + C$
4) $CO + C = C_2 + O$	11) $O + O = O_2^+ + e^-$
5) $C + O = CO^+ + e^-$	12) $CO + e^- = CO^+ + 2e^-$
6) $C + e^- = C^+ + 2e^-$	13) $O_2 + C^+ = O_2^+ + C$
7) $O + e^- = O^+ + 2e^-$	14) $O + O_2^+ = O^+ + O_2$

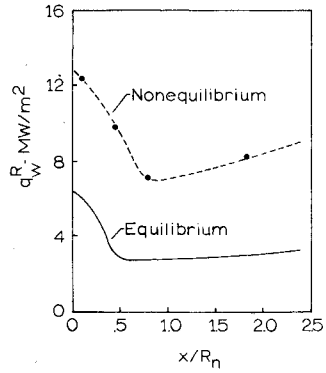

Fig. 3 Radiative heating rates to wall, 90.98 km.

equilibrium species concentrations and the effective electronic temperature, $T_{e_{CO}}$. Because the radiation in the nonequilibrium zone is dominated by the CO(4+) band system, all other radiating species were assumed to emit at $T_{e_{CO}}$.

An inconsistency arises in using the radiative transport code because free-free continua are calculated using a cross-section formulation which assumes chemical equilibrium between neutral atoms and their ions. By altering the code, calculations were made eliminating all ion free-free radiation and these results were then compared with the original calculations. This procedure indicated that the maximum error in the calculations due to the inconsistency would be less than 14%.

Figure 3 illustrates the calculated nonequilibrium radiative heating rates to the wall as a function of x/R_n for the 90.98 km alt case. For comparison the corresponding inviscid, equilibrium calculations[17] conducted by Sutton of the NASA Langley Research Center are also presented. Both curves have similar distributions but the nonequilibrium results are substantially higher due to the high temperature region near the shock front where the electronic temperature overshoot occurs. This produces enhanced radiative transfer to the body surface.

Several of the spectral profiles are shown in Fig. 4 for the $x/R_n = 0.116$ location. The spectral intensities close to the shock front ($y/y_b < 0.1$) are significantly different from those closer to the body. In the nonequilibrium zone the spectrum is dominated by the vacuum ultraviolet contributors—CO(4+) and C, O free-bound. As other species form and the temperature drops, the spectral profiles change so that the vacuum ultraviolet contribution is less pronounced. This behavior is primarily a temperature effect in the nonequilibrium zone. Figures 2b and 2c indicate that at the peak temperature ($\simeq$22,000 K), the CO concentration is still increasing and is approximately $\frac{1}{4}$ max value. The spectral profiles for other values of x/R_n show essentially the same behavior.

The calculations shown in Figs. 2–4 were done with a computational grid $\Delta x = 0.01$ m. The inviscid flowfield technique does not yield a solution at the stagnation point and provides better definition of flow properties across the shock layer as x/R_n increases. The location $x/R_n = 0.116$ ($x = 0.04$ m) was chosen as the closest location to the stagnation point at which there was sufficient definition of properties and species to perform the radiation calculations. Because the calculations were lengthy and required extensive computer time, the flowfield calculations were done with a computational grid four times coarser ($\Delta x = 0.04$ m) for the other three altitudes. The radiation calculations were performed only at $x/R_n = 0.466$ for these three altitudes. This location corresponds approximately to the minimum in the q_w^r vs x/R_n distribution.

Results

Figure 5 summarizes the results of the analysis by presenting the calculated nonequilibrium radiative heating rate to the body at various points in the mission trajectory. At the body location $x/R_n = 0.466$, the heating rate is shown as a function of altitude. For the 90.98 km alt case (near peak heating), the calculation at $x/R_n = 0.116$ is also shown. For comparison, the nonequilibrium results of Ref. 14 are presented. These heating rates were based on experimental normal shock studies conducted in a shock tube, in which nonequilibrium radiation profiles were observed behind normal shock waves for CO(4+) bands, carbon lines, and C_2 Swan bands. The normal shock wave profiles were related to blunt body flow by equating particle residence times in the shocked gas for these radiating species. (The particle residence time for the blunt body was

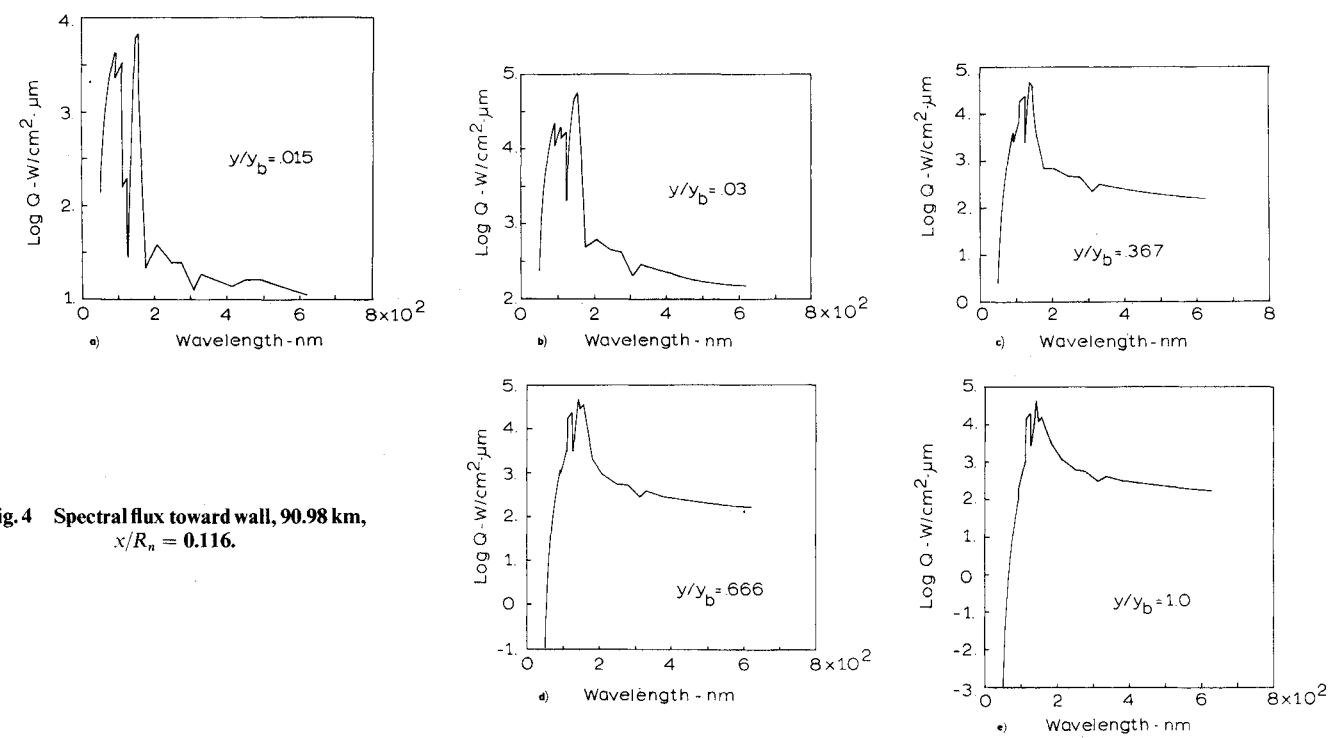

Fig. 4 Spectral flux toward wall, 90.98 km, $x/R_n = 0.116$.

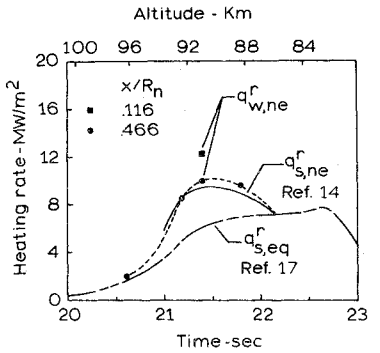

Fig. 5 Heating rates for large probe.

determined by assuming a linear velocity profile behind the bow shock.) It is apparent that the relative variation with altitude of the theoretical nonequilibrium results compares well with the shock tube studies. However, the absolute heating rate calculated for the stagnation region ($x/R_n = 0.116$) at 90.98 km is noticeably higher than the result from the shock tube studies. It is probable that the computational model tends to give results which are higher than a more exact model would yield, because the derived effective electronic temperature for CO was used to predict radiance from other species. The CO is formed first as CO_2 dissociates. The other species are formed later and their respective electronic temperatures would be expected to be somewhat lower.

In the shock tube studies, only CO(4+), C_2 swan band system, and C lines were monitored. It was assumed that all of the nonequilibrium radiation resulted from these sources. It would be expected then, that including more radiative contributors would cause the shock tube results to be somewhat higher than shown in Fig. 5.

For reference, inviscid equilibrium calculations of the cold-wall nonablating radiative heating rate to the stagnation point are also shown in Fig. 5. The peak nonequilibrium radiative contribution can be shown to occur at a point where the radiative heating is large and approximately equal to the convective heating. This result is in contrast to the results determined for Apollo.

Conclusions

The results of the present investigation of a described Venus mission indicate that nonequilibrium contributions to the radiative heating of the entry probe are of sufficient magnitude to warrant concern. At peak heating, the nonequilibrium radiative heating rate to the body is approximately twice the corresponding equilibrium value.

The results also confirm earlier investigations which conclude that radiation in the chemical nonequilibrium zone behind strong shock waves should be calculated using electronic temperatures for the radiating species. These temperatures are not related in a simple way to the local translational temperature.

References

[1] Page, W. A. and Arnold, J. O., "Shock Layer Radiation of Blunt Bodies at Reentry Velocities," TR R-193, 1964, NASA.

[2] Teare, J. D., Georgiev, S., and Allen, R. A., "Radiation From the Nonequilibrium Shock Front," Rept. 112, Oct. 1961, AVCO-Everett Research Lab., Everett, Mass.

[3] IIT Research Institute, "Radiative Energy Transfer on Entry into Mars and Venus," Rept. V6048, NASA Contract NASr-65(01), March 1969, IIT Research Institute, Annapolis, Md.

[4] Menard, W. A., Thomas, G. M., and Helliwell, T. M., "Experimental and Theoretical Study of Molecular, Continuum, and Line Radiation from Planetary Atmospheres," *AIAA Journal*, Vol. 6, April 1969, pp. 655–664.

[5] McKenzie, R. L. and Arnold, J. O., "Experimental and Theoretical Investigations of the Chemical Kinetics and Nonequilibrium CN Radiation Behind Shock Waves in CO_2–N_2 Mixtures," AIAA Paper 67-322, New Orleans, La., 1967.

[6] Ainsworth, J. E., "Comprehensive Study of Venus by Means of a Low-Cost Entry-Probe and Orbiter Mission-Series," Rept. X-625-70-203, 1970, also TM X-65423, 1970, NASA.

[7] Marcotte, P. G., "Planetary Explorer, Phase A Report and Universal Bus Description," TM X-67234, 1971, NASA.

[8] Goulard, R., "Preliminary Estimates of Radiative Transfer Effects on Detached Shock Layers," *AIAA Journal*, Vol. 2, March 1964, pp. 494–502.

[9] Grose, W. L., "A Thin-Shock-Layer Solution for Nonequilibrium, Inviscid Hypersonic Flows in Earth, Martian, and Venusian Atmospheres," TN D-6529, 1971, NASA.

[10] Maslen, S. H., "Inviscid Hypersonic Flow Past Smooth Symmetric Bodies," *AIAA Journal*, Vol. 2, June 1964, pp. 1055–1061.

[11] Avduevskii, V. S., Zavelevich, F. S., Marov, M. Y., Noikina, A. I., and Polezhaev, V. I., "Numerical Modeling of Radiative-Convective Heat Transfer in the Atmosphere of Venus," *Cosmic Research*, Vol. 9, No. 2, Oct. 1971, pp. 257–266.

[12] Evans, J. S., Schexnayder, C. J., Jr., and Grose, W. L., "Effects of Nonequilibrium Ablation Chemistry on Viking Radio Blackout," *Journal of Spacecraft and Rockets*, Vol. 11, Feb. 1974, pp. 84–88.

[13] Dunn, M. G., "Measurement of $C^+ + e^- + e^-$ and $CO^+ + e^-$ Recombination in Carbon Monoxide Flows," *AIAA Journal*, Vol. 9, Nov. 1971, pp. 2184–2190.

[14] Nealy, J. E. and Haggard, K. V., "A Shock Tube Study of Radiation Behind Shock Waves in CO_2 With Application to Venus Entry," Proceedings of the 9th International Shock Tube Symposium, Stanford Univ. Press, 1973, pp. 330–339.

[15] Hansen, C. F. and Chapin, C. E., "Nonequilibrium Radiation From the Stagnation Region of High-Velocity Bodies," Rept. TR 64-02G, Aug. 1964, General Motors Defense Research Labs., Santa Barbara, Calif.

[16] Nicolet, W. E., "User's Manual for the Generalized Radiation Transfer Code (RAD/EQUIL)," Aerotherm Rept. UM-69-9, Dec. 1969, Aerotherm Corp., Mountain View, Calif.; also CR-116353, 1970, NASA.

[17] Sutton, K., "Coupled Nongray Radiating Flow about Planetary Entry Bodies," *AIAA Journal*, Vol. 12, Aug. 1974, pp. 1099–1105.